

## RESEARCH ARTICLE

# Characterizing bracken fern phenological cycle using time series data derived from Sentinel-2 satellite sensor

Trylee Nyasha Matongera<sup>1</sup>\*, Onesimo Mutanga<sup>1</sup>, Mbulisi Sibanda<sup>2</sup>

**1** Discipline of Geography, University of KwaZulu-Natal, Scottsville, Pietermaritzburg, South Africa,

**2** Department of Geography, Environmental Studies and Tourism, University of Western Cape, Cape Town, South Africa

\* These authors contributed equally to this work.

\* [tryleematongera@gmail.com](mailto:tryleematongera@gmail.com)



## OPEN ACCESS

**Citation:** Matongera TN, Mutanga O, Sibanda M (2021) Characterizing bracken fern phenological cycle using time series data derived from Sentinel-2 satellite sensor. PLoS ONE 16(10): e0257196. <https://doi.org/10.1371/journal.pone.0257196>

**Editor:** Abel Chemura, Potsdam Institute for Climate Impact Research, GERMANY

**Received:** January 9, 2021

**Accepted:** August 25, 2021

**Published:** October 28, 2021

**Copyright:** © 2021 Matongera et al. This is an open access article distributed under the terms of the [Creative Commons Attribution License](https://creativecommons.org/licenses/by/4.0/), which permits unrestricted use, distribution, and reproduction in any medium, provided the original author and source are credited.

**Data Availability Statement:** The details for the data will be available after acceptance.

**Funding:** This work is funded by the National Research Foundation of South Africa (NRF) Research Chair initiative in Land Use Planning and Management (Grant Numbers: 84157). The funders had no role in study design, data collection and analysis, decision to publish, or preparation of the manuscript.

**Competing interests:** The authors have declared that no competing interests exist.

## Abstract

Bracken fern is an invasive plant that has caused serious disturbances in many ecosystems due to its ability to encroach into new areas swiftly. Adequate knowledge of the phenological cycle of bracken fern is required to serve as an important tool in formulating management plans to control the spread of the fern. This study aimed to characterize the phenological cycle of bracken fern using NDVI and EVI2 time series data derived from Sentinel-2 sensor. The TIMESAT program was used for removing low quality data values, model fitting and for extracting bracken fern phenological metrics. The Sentinel-2 satellite-derived phenological metrics were compared with the corresponding bracken fern phenological events observed on the ground. Findings from our study revealed that bracken fern phenological metrics estimated from satellite data were in close agreement with ground observed phenological events with  $R^2$  values ranging from 0.53–0.85 ( $p < 0.05$ ). Although they are comparable, our study shows that NDVI and EVI2 differ in their ability to track the phenological cycle of bracken fern. Overall, EVI2 performed better in estimating bracken fern phenological metrics as it related more to ground observed phenological events compared to NDVI. The key phenological metrics extracted in this study are critical for improving the precision in the controlling of the spread of bracken fern as well as in implementing active protection strategies against the invasion of highly susceptible rangelands.

## 1. Introduction

The encroachment of invasive species in productive rangelands influences changes in nutrient cycles [1], fire incidences and severity [2] and alters the abundance of biodiversity [3], resulting in socio-economic implications on livelihoods. Bracken (*Pteridium Aquilinum*) is one of the most problematic alien invasive ferns that encroaches into new landscapes [4]. In South Africa, there is evidence of bracken fern encroachment in the Drakensberg Mountains. Although it is not clear how bracken fern was introduced in the Drakensberg, Finch, Hill [5] noted that archeological evidence suggests that the existence of bracken fern in the Drakensberg montane

grasslands can be traced back to as far as 1840 CE. Due to its vigorous growth and dense canopy, the fern has negative impacts on agricultural productivity [6], animal and human health [7], forestry and recreational potential [8], leading to huge economic losses. Generally, farmers abandon the agricultural land once the fern heavily invades the land due to its persistent underground root system, which facilitates fast growth. The invasive fern invades grasslands and grazing pastures [9–11], while it also perseveres in woodlands and hedgerows, making it difficult for indigenous grass species to thrive [12]. Furthermore, the encroachment of bracken fern causes the reduction of herbaceous native vegetation and destruction of habitat in rangelands. The biochemical chemistry and morphology of bracken fern influence its spectral reflectance behavior. Specifically, bracken fern has various pigments and carotenoids pigments that forms part of the compound arrangement of the fern's cells which actively absorb and distribute radiation and different wavelengths [13].

Understanding the biological structure and timing of bracken fern phenology improves rangeland management's knowledge and ability to choose the suitable treatment method in areas infested by the fern [14]. The phenological information can be used to implement rapid response initiatives for the successful restoration of landscapes at different scales [14]. In literature, the prediction of future invasions before their occurrence has been postulated as one of the most efficient strategies of managing rangelands [15–17]. Therefore, understanding bracken fern phenology can help to predict how the fern species populations will change in time, and necessary proactive measures can be taken accordingly. Accurate and effective strategies in invasive species management save time and resources [18, 19]. A well-documented phenological cycle of bracken fern will assist conservationists and farmers in determining the most effective methods and appropriate time for controlling the fern across its life cycle stages, to ensure the complete eradication of the fern with minimum costs and inputs. For instance, knowing the beginning of the bracken fern season will help the rangeland managers with planning and implementing the appropriate control measures at an early phenological stage before the spores have been dispersed. Furthermore, the information on bracken fern's phenology is vital in understanding the major drivers of its population dynamics and patterns of invasion. In this regard, an understanding of bracken fern's phenological cycle will provide spatial information on areas that are more threatened for informing policy decisions on deriving effective control and management strategies. Over the past decades, remote sensing has proved to be an invaluable data source suitable for characterizing the phenological profile of vegetation at the local, regional and global scale [20–22]. Therefore, the uncontrolled colonization of bracken fern in the Drakensberg [23], ascertains the necessity to characterize its phenological cycle.

Earlier works on bracken fern phenology have used field-based studies [24, 25] and Phenology Cameras (PhenoCams) [26] to understand the phenological cycles of the fern in different parts of the world. However, the major limitation of these locally based methods is the spatial extent to which the plant phenological events were collected [27]. Remote sensing technology offers better prospects in providing archives of long term spatial data required to understand the phenological cycles of bracken fern at various scales. The use of remotely sensed data sets in retrieving the phenological metrics of vegetation is referred to as Land Surface Phenology (LSP) in remote sensing literature [28]. The application of remotely sensed data in estimating and monitoring LSP was pioneered by early satellite sensors such as Landsat series [29], Advanced Very High Resolution Radiometer (AVHRR) [30], the Moderate Resolution Imaging Spectroradiometer (MODIS) [31]. The AVHRR and MODIS satellite sensors have a high temporal resolution and synoptic views which is appropriate for large-scale monitoring of land surface phenology [30, 32, 33]. However, despite pioneering land surface phenology studies, the application of low spatial resolution sensors like AVHRR and MODIS is limited by their spatial resolution, calibration errors and poor geometric registration while Landsat is

limited by its low temporal resolution. The freely available Sentinel-2 Multi-Spectral Instrument (MSI) optical sensor is composed of two satellites; Sentinel-2A and 2B, hence its revisit time has been decreased from 10 to 3–5 days. The sensor has improved sensor calibration with 10 – 60m spatial resolution which presents a potential for successful characterization of the phenological cycles of vegetation at the species level.

LSP scientists have utilized numerous spectral vegetation indices derived from satellite data to estimate the phenological cycles of vegetation at various scales [34–38]. Over the past decades, vegetation indices were developed and used as indicators of changes in vegetation structure, density, spatial extent and phenological timings. The Normalized Difference Vegetation Index (NDVI) and the Enhanced Vegetation Index (EVI2) have been commonly used to quantify the cyclical patterns of vegetation in different ecosystems [39–43]. The NDVI is a commonly used vegetation index regarded as a proxy indicator of vegetation canopy function and is directly associated with the absorption of photosynthetically active radiation by plant canopies while EVI2 was developed to enhance the vegetation signal with better sensitivity in areas with high biomass [44].

The characterization of the phenological profile of specific vegetation species using satellite data has mainly been done for crops [45–48], whilst the estimation of the phenological cycles of specific invasive species such as bracken fern still requires more attention. To the best of our knowledge there are no published studies that have used polar orbiting satellite data sets such as Sentinel-2 to extract the phenological metrics of bracken fern for the purpose of improving its management approaches. Therefore, the first objective of this study was to characterize the phenological cycle of bracken fern using NDVI and EVI2 time series data derived from the Sentinel-2 satellite sensor. Secondly, the study sought to investigate the differences and similarities between NDVI and EVI2 data in estimating bracken fern phenological metrics. Finally, the study assessed the relationship between phenological metrics estimated from satellite data and the bracken fern phenological events recorded on the validation site, using Cathedral Peak World Heritage Site in the Drakensberg as the study site. This study is part of a continuing effort to craft an integrated approach to control the spread of invasive species in KwaZulu-Natal Nature reserves in South Africa.

## 2. Methods and materials

### 2.1 Study site description

The Cathedral Peak area is a World Heritage Site which falls within South Africa's summer rainfall region. The Drakensberg climate is a result of a combination of factors such as altitude, topography as well as the Agulhas current in conjunction with atmospheric pressure system patterns over and adjacent to South Africa [49]. The mean annual rainfall in the Drakensberg is approximately 1800mm [50]. The maximum daily temperatures exceed 25 degrees Celsius while the minimum daily temperatures may drop below 0 degrees Celsius during winter [51]. The area is characterized by a mountainous environment that is largely dominated by C<sub>3</sub> and C<sub>4</sub> grass species such as *Festuca* and *Themeda* respectively [52]. The Cathedral Peak landscape is also characterized by invasive species that are increasingly encroaching into the grasslands. Nearly seventy-five categories of alien invasive plants have been recorded to exist in Drakensberg [53]. Bracken fern is amongst the commonly found invasive species that have been invading rangelands in the Drakensberg.

### 2.2 Ground observed phenology data

The ground phenology recordings included the collection of bracken fern patches locations using a portable Leica GS20 Global Positioning System. A total of 60 bracken fern patches

were collected. The bracken fern patches that were recorded were larger than 10 by 10 m ( $100\text{m}^2$ ) for them to match the Sentinel-2-pixel size as well as to account for geolocation errors of the GPS and the Sentinel-2 imagery. Purposive sampling was used to select bracken fern patches with more than 75% bracken percentage cover. The bracken fern phenological developments were recorded weekly from 1 January 2016 to 31 December 2018. Ferns like bracken develop fronds instead of leaves, for ground phenology observations in this study, the term 'fronds' was used instead of leaves. Specifically, we recorded the dates of bracken fern frond emergence, expanded frond growth, withering and frond drying and considered them as green up, maturity, senescence and dormancy respectively. The recording of bracken phenological events on the ground was done with the assistance of the Department of Invasive Species for the Ezemvelo KwaZulu-Natal (KZN) Wildlife under the project licence number 144/2017b. There were no plants and animals that were destroyed or killed during then data collection process. Fig 1 shows the phenological transformation of bracken fern appearance from October 2016 to September 2017. The bracken fern photographs were captured weekly, but only monthly images were shown since they proved to be sufficient to show the change in the phenological appearance of the fern. For consistency, the photographs were captured in the same position, at a bracken fern patch located at  $29^{\circ}13'26.758''\text{E } 28^{\circ}56'46.2''\text{S}$ .

### 2.3 Satellite data acquisition and pre-processing

Sentinel-2 Multispectral Instrument (MSI) satellite images were obtained from the European Space Agency (ESA) online platform (<https://earthexplorer.usgs.gov/>). Sentinel-2A and 2B satellite images were included in the time series data for bracken fern phenological analysis. The satellite images were acquired at the processing level 1C. The images were atmospherically and geometrically corrected by ESA. A total of 108 images from January 2016 to December 2018 were acquired. Sentinel-2 images with less than 20% cloud cover were selected and included in the phenological analysis. The Function of mask (Fmask) 4.0 algorithm was used for detecting and removing clouds and shadows in the satellite images. For more details about the Fmask 4.0 algorithm procedure, see Qiu, Zhu [54].



**Fig 1. Phenological transformation of bracken fern appearance from October 2016 to September 2017 captured in Cathedral Peak study site.**

<https://doi.org/10.1371/journal.pone.0257196.g001>

The Normalized Difference Vegetation Index (NDVI) [55] and the two band Enhanced Vegetation Index (EVI2) [56] were used to extract the bracken fern phenological metrics. The NDVI was chosen based on its long term successfully applications in the phenology studies [57–59]. NDVI is suitable for both local and large-scale vegetation assessments, related to canopy structure and canopy photosynthesis, an attribute that is very crucial in the current study. EVI2 was also used based on its sensitivity to coherent inter-band (blue, red and NIR) atmospheric correction and thus may become much better over extreme bright or dark surfaces, such as subpixel clouds, desert playas, and inland water bodies, where the EVI values are usually problematic [60]. Additionally, EVI2 has also been reported to solve resolve Leaf area Index (LAI) differences for vegetation with different background soil reflectance [61]. The NDVI and EVI2 indices were calculated using the 108 Sentinel-2A and 2B satellite images in the TerrSet Geospatial Monitoring and Modelling System (Version 18.21) software based on the following equations:

$$\text{NDVI} = (\text{NIR} - \text{RED}) / (\text{NIR} + \text{RED}) \quad \text{Eq (1)}$$

$$\text{EVI2} = G (\text{NIR} - \text{Red}) / (\text{NIR} + (6 - 7.5/C) \text{Red} + 1) \quad \text{Eq (2)}$$

where NIR, red and blue represents the quantity of NIR, red and blue light reflected by vegetation and measured by the satellite sensor [62], 2.5 is the gain or scaling factor; 6 and 7.5 are coefficients of the aerosol resistance term while 1 represents the canopy background adjustment for correcting the nonlinear, differential NIR and red radiant transfer through a canopy. G will be determined in accordance with the c value. The NDVI and EVI2 images were exported to TIMESAT program for further analysis.

## 2.4 Data smoothing and phenological metrics extraction

The current study used TIMESAT 3.3 program for processing vegetation indices time series data and estimating bracken fern phenological metrics. The TIMESAT program provides an understandable Matlab based user interface which facilitates the manipulation of data into vegetation phenological parameters. Specifically, three main processing stages were executed in TIMESAT: (1) preprocessing of NDVI and EVI2 time series data by detecting and removing outliers, (2) data smoothing and gap filling using the SG, DL and AG models based on the procedures which are described in detail by Eklundha and Jönsson [63] and (3) extraction of bracken fern phenological metrics. Fig 2A and 2B show the temporal trajectory of raw and smoothed NDVI and EVI2 time series respectively from 2016 to 2018 for a pixel located in the Cathedral Peak at co-ordinates (29° 13' 26.758" E 28° 56' 46.2" S). To provide the most robust description of bracken fern seasonal dynamics, 10-fold leave one out cross validation was used to automatically select the smoothing parameters for the SG, AG and DL smoothing functions as described in detail by Craven and Wahba [64].

In the current study, the bracken fern growth cycle was characterized by four main transition dates which are; 1) green up: indicating the date of onset of vegetation indices increase, 2) maturity: the date indicating the onset of vegetation indices maximum, 3) senescence: the date of onset of vegetation indices decrease and 4) dormancy: the date of onset of vegetation minimum. The TIMESAT program relies on the assumption that the growing seasons begin and end at a similar time annually. In principle, the start and end of the season for the targeted year is identified in the same time period as the first and third years [33]. The seasonal amplitude threshold method was used to extract bracken fern phenological metrics. The seasonal amplitude method is defined between the base level and the maximum value for each individual season [63]. The principle of the seasonal amplitude method states that the start of the



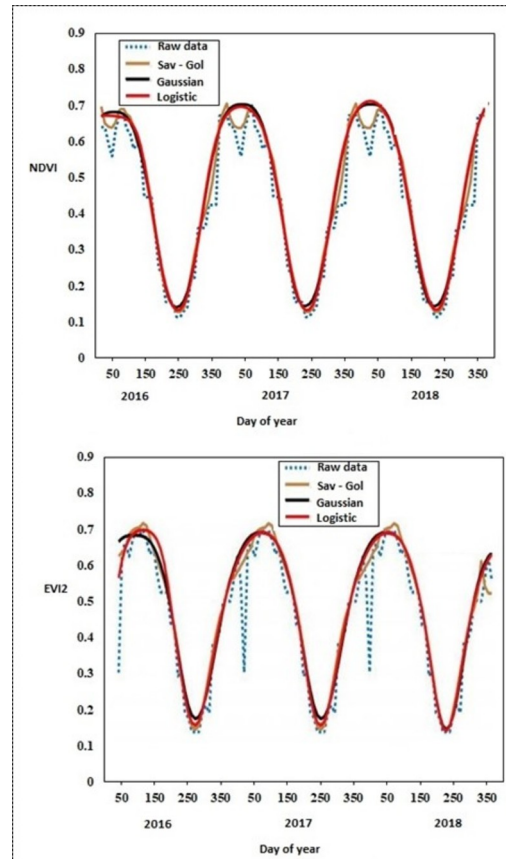


**Fig 2.** Graphical representation of (a) NDVI and (b) EVI2 raw and fitted time series data computed using SG, DL and AG models for a bracken fern pixel located in Cathedral Peak (29°13'26.758"E 28°56'46.2"S).

<https://doi.org/10.1371/journal.pone.0257196.g002>

season occurs when the left section of the fitted curve has reached a specified fraction of the amplitude, which is counted from the base level. The end of the season is also defined similarly but using the right side of the fitted curve. In this study, the start of the bracken fern season was defined as the day of the year when the vegetation indices surpassed 10% of the distance between the left minimum level and the maximum, while the end of the season is defined in a similar way, but in the opposite direction. For more details about the threshold fraction specifications, see the original technical paper by Jönsson and Eklundh [65].

## 2.5 Statistical analysis

To assess the statistical relationships between satellite-derived phenological metrics and ground observed bracken fern phenological events, the coefficient of determination ( $R^2$ ) [66], the Root Mean Square Deviation (RMSD) [67] and the Mean Absolute Bias (MAB) [68] were computed. For comparison between satellite retrieved and ground observed phenological dates, the linear regression analysis was computed by using the ground observed phenological events as the independent variable and the satellite-derived vegetation indices as the dependent variable. The linear regression analysis was also conducted between NDVI and EVI2 phenological retrievals with NDVI and EVI2 retrievals as independent and dependent variables, respectively. The significance test for all the phenology models were conducted using the F-test with the standard 0.05 cut off indicating statistical significance between variables ( $P < 0.05$ ). Fig 3 shows the flow chart illustrating the research methodology that was adopted in this study.

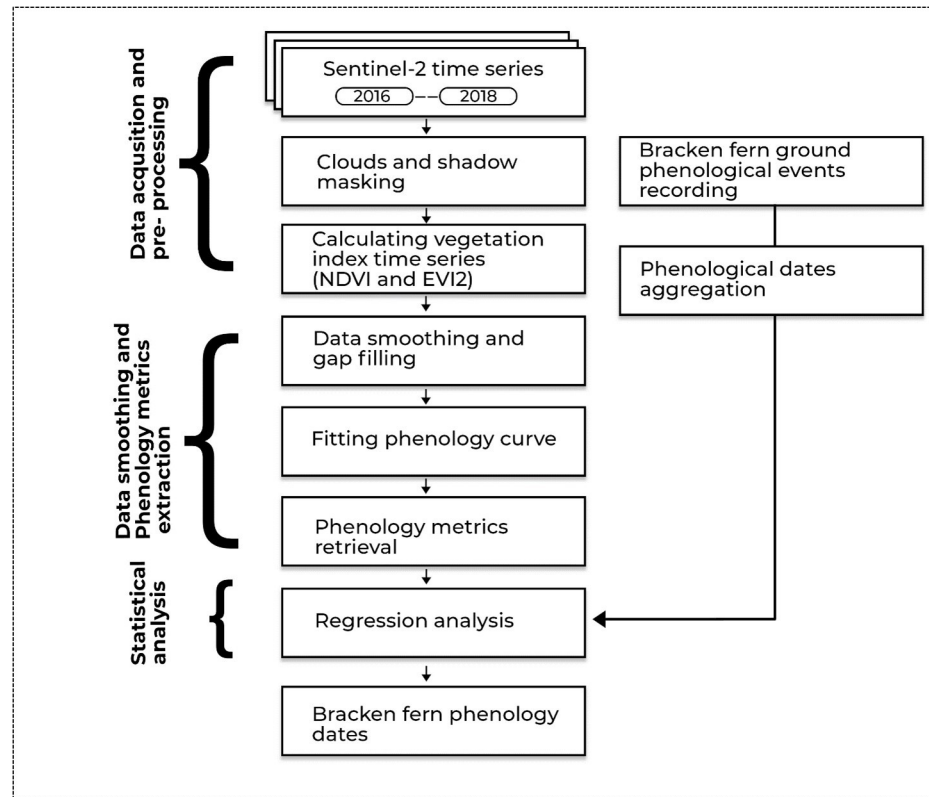


Fig 3. Schematic diagram illustrating the research methodology adopted in this study.

<https://doi.org/10.1371/journal.pone.0257196.g003>

### 3. Results

#### 3.1 Variation in TIMESAT models phenological retrievals

Table 1 shows a summary of bracken fern phenological metrics computed from the three models embedded in the TIMESAT program. Comparison of the mean phenological dates estimated using the three models revealed that bracken fern phenological dates from each model were different although their discrepancies were all less than 15 days. The statistical analysis revealed that the variance in the estimated phenological dates produced by the three models were statistically significant ( $p < 0.05$ ) for all the bracken fern phenological stages based on both NDVI and EVI2 time series. Results obtained using NDVI phenological retrievals shows that the mean bracken fern green up onset dates for the AG, SG and the DL were approximately around day 298, 296 and 294 while EVI2 dates were estimated to be around day 280, 288 and 284 respectively. Using the calendar dates, the average timing of bracken fern green up onset dates was towards the end of October 2016. The EVI2 green up onset dates were generally earlier than NDVI dates by an average of 11 days across the three models. For all the models, the standard deviations for the green up onset retrievals were consistent with a range of 2 to 5 days. Based on the NDVI phenological estimations, the DL model recorded the lowest deviation of 2.96 days while the SG NDVI model reported the highest deviation of 5.3 days.

The NDVI maturity onset dates for the AG, SG and the DL were estimated to have occurred around day 54, 57 and 56 while the EVI2 dates were predicted to be around day 44, 53 and 54 respectively. Using the calendar dates, the estimated bracken fern maturity dates were towards the end of February 2017. The NDVI maturity onset dates were later than EVI2 dates by an

**Table 1. Mean phenological dates and standard deviations for the three models embedded in TIMESAT.**

Model	Phenological metric	Mean (DOY)		Calendar Date	Standard Deviation (Days)	
		NDVI	EVI2		NDVI	EVI2
SG	GU	296	288	October; 2016	5.3	3.78
	MAT	57	53	February; 2017	3.36	3.04
	SEN	101	88	April; 2017	5.36	3.91
	DM	176	196	July; 2017	2.03	2.52
DL	GU	294	284	October; 2016	4.96	2.96
	MAT	56	54	February; 2017	3.86	2.56
	SEN	99	90	April; 2017	3.69	2.92
	DM	177	184	July; 2017	6.23	4.38
AG	GU	298	280	October;2016	3.76	4.73
	MAT	54	44	February;2017	6.11	7.35
	SEN	96	88	April;2017	3.34	2.57
	DM	181	190	July;2017	5.59	3.82

where GU = green up; MAT = maturity; SEN = senescence; DM = dormancy.

<https://doi.org/10.1371/journal.pone.0257196.t001>

average of 8 days across the three models. Compared to the green up the phenological stage, the maturity standard deviations were higher across all the models ranging from 2 to 7 days. The bracken fern green decrease was associated with the plummet in the vegetation index signal which signified the onset of the senescence phenological stage. Based on the AG, DL and SG the NDVI estimated date of senescence onset was around day 96, 99 and 101 while EVI2 retrievals estimated day 88, 90 and 81 respectively. The standard deviations ranged from 2 to 5 days across all models. The NDVI retrievals predicted the onset of dormancy stage to be around day 181, 177 and 176 for AG, DL and SG, while EVI2 retrievals were estimated to be around day 190, 184 and 196 respectively. For both NDVI and EVI2 phenological retrievals, the DL dormancy dates were earlier when compared to the other two models by an average of 16 days. The SG model had the lowest standard deviations (NDVI = 2.03 and EVI2 = 2.52), while the DL recorded the highest deviations (NDVI = 6.23 and EVI2 = 3.42).

### 3.2 Intercomparison of NDVI and EVI2 phenological retrievals

To compare bracken fern phenological metrics retrieved using NDVI and EVI2 time series, we averaged the dates of the four metrics estimated using the three models embedded in TIMESAT. Findings from our study demonstrated that the phenological metrics estimated using NDVI and EVI2 across the four major bracken fern phenological stages were comparable. The statistical analysis on Fig 4 shows scatter plots depicting the agreement between bracken phenological metrics estimated using the two vegetation indices. The EVI2 and NDVI phenological metrics show significant linear relationships between each other amongst all phenological stages ( $p < 0.05$ ) although the correlation coefficients were weak for some of the phenological stages with  $R^2$  values ranging from 0.49–0.61. For the green up onset stage, the coefficient of determination ( $R^2 = 0.58$ ) indicated a good correlation between NDVI and EVI2 phenological retrievals. The EVI2 phenological dates for green up onset were earlier than NDVI retrievals for most of the pixels across the study site. The green up onset RMSD was 8.2 days while a bias of 4.9 days was recorded.

The maturity stage recorded the lowest correlation between NDVI and EVI2 phenological retrievals ( $R^2 = 0.49$ ), the highest RMSD (9.8 days) as well as the highest bias of 5.6 days. Like the green up onset dates, the EVI2 retrievals recorded earlier green up onset dates compared



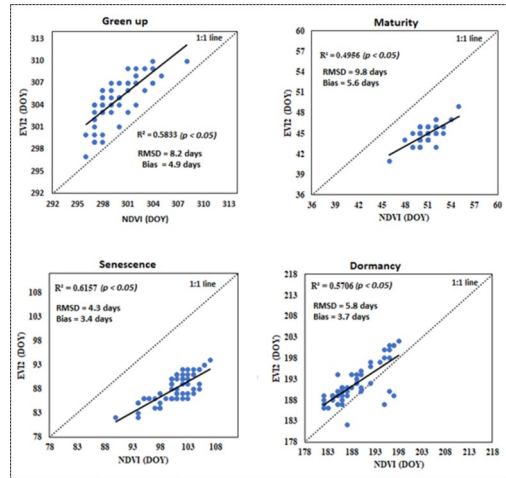


**Fig 4. Statistical comparison between NDVI and EVI2 derived bracken fern phenological dates.**

<https://doi.org/10.1371/journal.pone.0257196.g004>

to the NDVI retrievals. The senescence stage recorded a good correlation ( $R^2 = 0.61$ ) for the phenological retrievals between the two vegetation indices and a relatively moderate RMSD of 4.3 days and a bias of 3.4 days. The highest correlation between NDVI and EVI2 phenological retrievals was reported in the dormancy phenological stage ( $R^2 = 0.57$ ) while the RMSD recorded 5.8 days and bias was 3.7 days. Generally, the agreement was moderate, and bias was low between phenological metrics estimated using the two vegetation indices across the four bracken fern phenological stages. The EVI2 phenological retrievals were mostly earlier than NDVI retrievals across the four bracken fern phenological stages.

### 3.3 Comparison between satellite-based phenological retrievals and ground observations

Bracken fern phenological metrics estimated using NDVI and EVI2 generally showed a good agreement with phenological dates from ground observations. Both EVI2 and NDVI phenological metrics show significant linear relationships ( $p < 0.05$ ) with bracken fern ground observed phenological events with varying correlations across all phenological stages. To provide a more comprehensive and quantitative assessment, Fig 5 shows scatter plots illustrating the statistical agreement between satellite-derived phenological metrics and ground observed

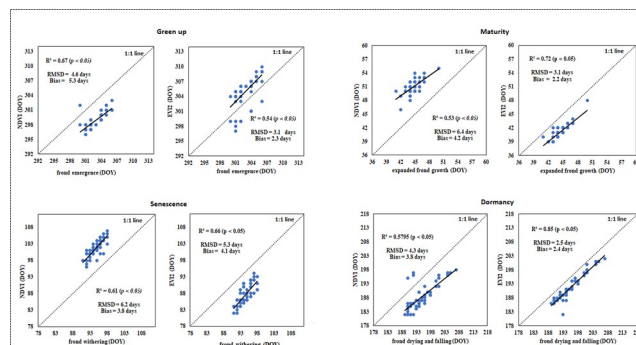


**Fig 5. Statistical comparison between satellite-derived bracken fern phenological dates and ground observed phenology.**

<https://doi.org/10.1371/journal.pone.0257196.g005>

transitional dates. The coefficients of determination for both NDVI and EVI2 phenological retrievals indicated a correlation with ground observed onset dates, with  $R^2$  values ranging from 0.53–0.85. The dormancy<sub>EVI2</sub> phenological retrievals recorded the highest correlation ( $R^2 = 0.85$ ) with the ground observed frond drying and falling dates. The relationship between EVI2 retrieved dormancy onset dates and the ground observed bracken fern frond drying and falling showed a very strong correspondence for more than 75% of the pixels across the study site. The maturity<sub>EVI2</sub> also reported a strong correspondence ( $R^2 = 0.72$ ) with ground observed bracken fern expanded frond growth.

The RMSDs statistical values between satellite-based phenological retrievals and ground observed phenological transitional dates ranged from 2.5 to 6.4 days across the four bracken fern phenological stages. The RMSDs between NDVI and corresponding ground transitional dates were modestly higher (approximately one week) for senescence and dormancy phenological stages, while the EVI2 maturity and dormancy had the lowest RMSDs of 3.1 and 2.4 days respectively. The RMSDs between NDVI and ground recorded phenological dates were also higher (approximately one week) for maturity, senescence and dormancy while the green up phenological stage showed the lowest RMSD value of 4.6 days. The bias between satellite-based phenological retrievals and ground observed phenological events appeared to be very low as they ranged from 2.2 to 5.3 days. The largest bias (5.3 days) was recorded between green up<sub>NDVI</sub> bracken fern frond withering, while the lowest bias (2.2 days) was reported between maturity<sub>EVI2</sub> and bracken fern frond emergence. Generally, the EVI2 phenological retrievals corresponded more with bracken fern ground observed phenological events compared to NDVI phenological retrievals as shown by higher EVI2 correlation coefficients and lower RMSDs and Biases. Overall, the satellite-based bracken fern phenological estimates matched moderately well with the ground observed phenological events.

## 4. Discussion

### 4.1 The role of remotely sensed data in characterizing bracken fern phenology

The current study characterized the phenological cycle of bracken fern invasive species using NDVI and EVI2 time series data derived from the Sentinel-2 MSI sensor. The satellite-based phenological retrievals were compared with bracken fern ground observed phenological events. The Sentinel-2 sensor proved to be a reliable data source that could assist in improving the understanding of bracken fern phenological cycles, an aspect that could lead to better management of rangelands that are infected by the fern. Corresponding to our findings in this study, a plethora of scientific studies have also reported the capability of Sentinel-2 data in extracting the phenological cycles of vegetation at various scales [34, 69–71]. Since Drakensberg is not prone to high cloud coverage, the sensor's revisit time was sufficient to adequately capture the phenological changes of bracken fern. However, slight cloud coverage issues were experienced during the bracken fern maturity stage which coincided with the peak of the summer season. This could explain lower correlations between NDVI and bracken fern ground observed phenological events during the bracken fern maturity phenological stage.

The bracken fern phenological metrics estimated using the three models in the TIMESAT program were comparable across the four bracken fern phenological stages. The shape of the fitted NDVI and EVI2 curves in Fig 4 shows a possible quick response to precipitation, followed by a slow decay as bracken fern fronds withered. Corresponding with findings reported by Eklundh and Jönsson [72], our study established that the DL and AG models produced phenological curves that were subsequently used to estimate bracken fern phenological metrics that were more correlated to ground observed phenological events as compared to the SG

model. Similarly, the works of Cai, Jönsson [73] also concluded that the AG and DL models produced a more robust and accurate description of the phenological cycles of vegetation compared to the other methods tested in their study including the SG model. Although the AG and DL produced similar bracken fern phenological curves, it can be noted that the AG well adapts and performs better during vegetation indices peaks as compared to the DL model. The works of Tan, Morisette [34] reported that the AG is less affected by noise and has a great advantage if the time series data has missing data or if the satellite data is poor quality due to sensor calibration errors. SG is mostly affected by atmospheric impurities and subsequently produces erroneous phenological metrics especially during the peak of the season where the data is characterized by clouds. Results from our study corresponded with previous findings by Li and Liu [74] and Khobkhun, Prayote [75] who reported that the SG model works well for data that is unaffected by noise caused by atmospheric contamination. Generally, our study demonstrated that the three models in TIMESAT perform good and they can reduce noise, reconstruct, and fit time series data for the estimation of bracken phenological metrics. However, the tuning of parameters is essential in the extraction of phenological metrics using these three models. The inappropriate selection of parameters may lead to uncertainty and bias in phenological trends produced by data smoothing models. The tuning of parameters in phenological metrics extraction was also raised in literature by Stanimirova, Cai [76] who highlighted that the differences in tuning parameters such as the use of 10% or 15% of seasonal amplitude as a benchmark threshold to ascertain the phenological metrics will yield different results.

#### 4.2 Comparisons with ground observed phenological events

The validation of phenology metrics is essential for the evaluation of satellite sensors' performance in estimating LSP. However, previous research studies have shown that the validation of remote sensing products is a huge challenge in LSP investigations [77–79]. Overall, the EVI2 performed better in estimating bracken fern phenological metrics that were correlated to ground observed phenological events. EVI2 proved to produce better estimates that are comparable to bracken fern ground observations during the maturity, senescence and dormancy phenological stages. Corresponding with our findings, Peng, Wang [80] noted that EVI2 significantly improves linearity with biophysical vegetation properties and reduces saturation effects found in densely vegetated surfaces, a challenge which is commonly encountered when using NDVI. Similarly, Zhang, Jayavelu [37] concluded that EVI2 is the better choice for detecting phenology than NDVI because EVI2 phenological retrievals were in close agreement with PhenoCam observations. The performance of EVI2 could also be attributed to its resistance to soil background effects which normally causes artificial increase in NDVI as reported by Rocha and Shaver [60]. On the other hand, NDVI outperformed EVI2 in retrieving the bracken fern green up onset. The performance of NDVI in estimating the onset of bracken fern green up could be attributed to its ability to reduce topographic effects [81] and illumination conditions [82] much better as compared to the EVI2.

The NDVI showed poor correlation with ground observation during the maturity phenological stage, while the EVI2 retrievals performed well during the maturity stage. As the bracken fern fronds increased in size and the canopy expanded, NDVI tends to saturate and become less efficient in extracting phenological metrics during the maturity period. The differences in phenological retrievals between NDVI and EVI2 probably originated from various resistance levels to noise and sensitivities to spectral signal at different bracken fern stage of the growing season. The NDVI's poor performance in estimating the bracken fern maturity could probably be related to its loss of sensitivity when vegetation canopy's leaf area index reaches a maximum as reported by Davi, Soudani [83] and Soudani, François [84]. Our results

were consistent with Zuo, Liu [85] and Zhao, Yang [86] who reported that NDVI has more ability to track weak spectral signals in the early and end of vegetation growth season and tends to saturate at dense vegetation. Findings from the current study are consistent with previous work by Pettorelli, Vik [87] who noted that false highs occur when high NDVI values are considered to give better estimations than low values, and the bias tends to break the assumptions of many standard statistical methods. The rapid changes of NDVI during the bracken fern maturity period makes it complex for the determination of the phenological metrics. A study by Tan, Morisette [33] confirmed that vegetation normally changes quickly during green up and maturity, making it difficult to accurately detect changes in NDVI fluctuations.

### 4.3 Implications to the control and management of bracken fern

Challenges in controlling the encroachment of bracken fern into areas of ecological importance due to inappropriate timing, have been widely reported in literature [6, 13, 88, 89]. Therefore, the accurate estimation of bracken fern phenological transition times will help in the appropriate timing control measures and efforts of controlling the invasive fern for better management of the rangelands. Furthermore, the information on bracken fern's phenology is vital in understanding the major drivers of its population dynamics and patterns of invasion. The effective management of rangelands requires continuous data sources that track the changes in various vegetation species that are within a landscape. Dawson, Jackson [90] highlighted that an effective conservation response must be broadly coordinated and informed by a range of scientific approaches with diverse data sources. The free availability of high spatial and temporal resolution data sets such as Sentinel-2 enables rangeland managers to continuously monitor the changes that occur within areas of their jurisdiction.

The debate with regards to the most suitable methods of controlling the spread of bracken fern has received much attention in the literature [13, 91, 92]. Findings from the current study suggest that the Sentinel-2 data is an invaluable tool that can be used as a foundation for decision-making particularly in controlling the spread of bracken fern in ecologically sensitive areas. The current study suggests that the development of bracken fern spores at the beginning of the senescence phase can be timely controlled using chemical measures such as spraying with asulum before they disperse. The application of chemicals on bracken fern during the senescence period significantly reduces the number of fronds that will be produced the following season [24]. Asulum does not affect in the year of application but kills almost all the buds on the rhizome which leads to less production of fronds in the following growing season. The mechanical control methods would probably be suitable during the green up phase when the bracken frond biomass is still low.

## 5. Conclusions and future works

The current study focused on characterizing the phenological cycle of bracken fern using NDVI and EVI2 time series data derived from the Sentinel-2 sensor. The satellite-based phenological retrievals showed a good correlation with bracken fern ground observed phenological events, making remote sensing technology a potential tool for effective bracken fern management. Inter-comparisons between NDVI and EVI2 based phenological metrics revealed that the two vegetation indices differ in their ability to track the phenological developments of bracken fern during its growing season. EVI2 is more suitable for retrieving LSP metrics than NDVI as it produced phenological metrics that were more related to bracken fern ground phenological events. The AG and DL models produced the best fits that optimally described the phenological profile of bracken fern. Through this study, remote sensing has been demonstrated to be an invaluable data source that can be used by conservationists,

ecologists and rangeland managers in controlling and managing bracken-infested rangelands. The key phenology dates derived from the Sentinel-2 time series are relevant in informing stakeholders and policymakers on designing effective management strategies for controlling bracken fern invasion. After the successful characterization of bracken fern phenological cycle in the Drakensberg, the bracken fern phenological data may be used to improve the management of rangelands.

## Acknowledgments

The authors would like to thank the Ezemvelo KwaZulu-Natal Wildlife officials for their assistance during field data collection.

## Author Contributions

**Data curation:** Trylee Nyasha Matongera.

**Investigation:** Trylee Nyasha Matongera.

**Methodology:** Trylee Nyasha Matongera.

**Software:** Trylee Nyasha Matongera.

**Supervision:** Onesimo Mutanga.

**Writing – original draft:** Trylee Nyasha Matongera.

**Writing – review & editing:** Mbulisi Sibanda.

## References

1. Zhao C-Y, Liu Y-Y, Shi X-P, Wang Y-J. Effects of soil nutrient variability and competitor identify on growth and co-existence among invasive alien and native clonal plants. *Environmental Pollution*. 2020; 261:113894. <https://doi.org/10.1016/j.envpol.2019.113894> PMID: 32062457
2. Gharari R, Kazeminejad H, Kojouri NM, Hedayat A. A review on hydrogen generation, explosion, and mitigation during severe accidents in light water nuclear reactors. *International Journal of Hydrogen Energy*. 2018; 43(4):1939–65.
3. Linders TEW, Schaffner U, Eschen R, Abebe A, Choge SK, Nigatu L, et al. Direct and indirect effects of invasive species: Biodiversity loss is a major mechanism by which an invasive tree affects ecosystem functioning. *Journal of Ecology*. 2019; 107(6):2660–72.
4. Ngubane Z, Odindi J, Mutanga O, Slotow R. Assessment of the contribution of WorldView-2 strategically positioned bands in Bracken fern (*Pteridium aquilinum* (L.) Kuhn) mapping. *South African Journal of Geomatics*. 2014; 3(2):210–23.
5. Finch JM, Hill TR, Meadows ME, Lodder J, Bodmann L. Fire and montane vegetation dynamics through successive phases of human occupation in the northern Drakensberg, South Africa. *Quaternary International*. 2021.
6. Berget C, Duran E, Bray DB. Participatory restoration of degraded agricultural areas invaded by bracken fern (*Pteridium aquilinum*) and conservation in the Chinantla Region, Oaxaca, Mexico. *Human ecology*. 2015; 43(4):547–58.
7. Senyanzobe J, Mulei J, Bizuru E, Books R, OER R, SCARDA R, et al., editors. Environmental and social impacts of *Pteridium aquilinum* (L.) Kuhn (Bracken Fern) invasive species growing in Nyungwe Forest, Rwanda. Fifth African Higher Education Week and RUFORUM Biennial Conference 2016, "Linking agricultural universities with civil society, the private sector, governments and other stakeholders in support of agricultural development in Africa", Cape Town, South Africa, 17–21 October 2016; 2016: RUFORUM.
8. Ssali F, Moe SR, Sheil D. A first look at the impediments to forest recovery in bracken-dominated clearings in the African Highlands. *Forest Ecology and Management*. 2017; 402:166–76.
9. Sato Y, Mashimo Y, Suzuki RO, Hirao AS, Takagi E, Kanai R, et al. Potential Impact of an Exotic Plant Invasion on Both Plant and Arthropod Communities in a Semi-natural Grassland on Sugadaira Montane in Japan. *Journal of Developments in Sustainable Agriculture*. 2017; 12(1):52–64.



10. Maya-Elizarrarás E, Schondube JE. Birds, cattle, and bracken ferns: bird community responses to a Neotropical landscape shaped by cattle grazing activities. *Biotropica*. 2015; 47(2):236–45.
11. Hamer U, Potthast K, Burneo JI, Makeschin F. Nutrient stocks and phosphorus fractions in mountain soils of Southern Ecuador after conversion of forest to pasture. *Biogeochemistry*. 2013; 112(1):495–510.
12. Odindi JO, Adam EE, Ngubane Z, Mutanga O, Slotow R. Comparison between WorldView-2 and SPOT-5 images in mapping the bracken fern using the random forest algorithm. *Journal of Applied Remote Sensing*. 2014; 8(1):083527.
13. Matongera TN, Mutanga O, Dube T, Lottering RT. Detection and mapping of bracken fern weeds using multispectral remotely sensed data: a review of progress and challenges. *Geocarto international*. 2018; 33(3):209–24.
14. Taylor RV, Holthuijzen W, Humphrey A, Posthumus E. Using phenology data to improve control of invasive plant species: A case study on Midway Atoll NWR. *Ecological Solutions and Evidence*. 2020; 1(1): e12007.
15. Fournier A, Penone C, Pennino MG, Courchamp F. Predicting future invaders and future invasions. *Proceedings of the National Academy of Sciences*. 2019; 116(16):7905–10. <https://doi.org/10.1073/pnas.1803456116> PMID: 30926662
16. Jazwa M, Jedrzejczak E, Klichowska E, Pliszko A. Predicting the potential distribution area of *Solidago xniederederi* (Asteraceae). *Turkish Journal of Botany*. 2018; 42(1):51–6.
17. Fletcher D, Gillingham P, Britton J, Blanchet S, Gozlan RE. Predicting global invasion risks: a management tool to prevent future introductions. *Scientific reports*. 2016; 6(1):1–8. <https://doi.org/10.1038/s41598-016-0001-8> PMID: 28442746
18. Courtois P, Figuières C, Mulier C, Weill J. A cost–benefit approach for prioritizing invasive species. *Ecological Economics*. 2018; 146:607–20.
19. Baker CM, Bode M. Placing invasive species management in a spatiotemporal context. *Ecological Applications*. 2016; 26(3):712–25. <https://doi.org/10.1890/15-0095> PMID: 27411245
20. Wang J, Yang D, Detto M, Nelson BW, Chen M, Guan K, et al. Multi-scale integration of satellite remote sensing improves characterization of dry-season green-up in an Amazon tropical evergreen forest. *Remote Sensing of Environment*. 2020; 246:111865.
21. Bolton DK, Gray JM, Melaas EK, Moon M, Eklundh L, Friedl MA. Continental-scale land surface phenology from harmonized Landsat 8 and Sentinel-2 imagery. *Remote Sensing of Environment*. 2020; 240:111685.
22. Small C, Sousa D. Spatiotemporal characterization of mangrove phenology and disturbance response: the Bangladesh Sundarban. *Remote Sensing*. 2019; 11(17):2063.
23. Matongera TN, Mutanga O, Dube T, Sibanda M. Detection and mapping the spatial distribution of bracken fern weeds using the Landsat 8 OLI new generation sensor. *International journal of applied earth observation and geoinformation*. 2017; 57:93–103.
24. Pakeman R, Marrs R, Jacob P. A model of bracken (*Pteridium aquilinum*) growth and the effects of control strategies and changing climate. *Journal of applied ecology*. 1994:145–54.
25. Williams G, Foley A. Seasonal variations in the carbohydrate content of bracken. *Botanical Journal of the Linnean Society*. 1976; 73(1–3):87–93.
26. Granados JA, Graham EA, Bonnet P, Yuen EM, Hamilton M. EcoIP: An open source image analysis toolkit to identify different stages of plant phenology for multiple species with pan–tilt–zoom cameras. *Ecological informatics*. 2013; 15:58–65.
27. Matongera TN, Mutanga O, Sibanda M, Odindi J. Estimating and Monitoring Land Surface Phenology in Rangelands: A Review of Progress and Challenges. *Remote Sensing*. 2021; 13(11):2060.
28. Bornez K, Descals A, Verger A, Peñuelas J. Land surface phenology from VEGETATION and PROBA-V data. Assessment over deciduous forests. *International Journal of Applied Earth Observation and Geoinformation*. 2020; 84:101974.
29. Rea J, Ashley M. Phenological evaluations using Landsat—1 sensors. *International Journal of Biometeorology*. 1976; 20(3):240–8.
30. Justice CO, Townshend J, Holben B, Tucker eC. Analysis of the phenology of global vegetation using meteorological satellite data. *International Journal of Remote Sensing*. 1985; 6(8):1271–318.
31. Zhang X, Friedl MA, Schaaf CB, Strahler AH, Hodges JC, Gao F, et al. Monitoring vegetation phenology using MODIS. *Remote sensing of environment*. 2003; 84(3):471–5.
32. Reed BC, Brown JF, VanderZee D, Loveland TR, Merchant JW, Ohlen DO. Measuring phenological variability from satellite imagery. *Journal of vegetation science*. 1994; 5(5):703–14.
33. Tan B, Morissette JT, Wolfe RE, Gao F, Ederer GA, Nightingale J, et al. An enhanced TIMESAT algorithm for estimating vegetation phenology metrics from MODIS data. *IEEE Journal of Selected Topics in Applied Earth Observations and Remote Sensing*. 2011; 4(2):361–71.

34. Vrieling A, Meroni M, Darvishzadeh R, Skidmore AK, Wang T, Zurita-Milla R, et al. Vegetation phenology from Sentinel-2 and field cameras for a Dutch barrier island. *Remote Sensing of Environment*. 2018; 215:517–29.
35. Fernández-Manso A, Fernández-Manso O, Quintano C. SENTINEL-2A red-edge spectral indices suitability for discriminating burn severity. *International journal of applied earth observation and geoinformation*. 2016; 50:170–5.
36. Michele V, Roshanak M, Tiejun S, Raul W, Kees Z-M, Brian O. Vegetation phenology from Sentinel-2 and field cameras for a Dutch barrier island. *Remote sensing of environment*. 2018.
37. Zhang X, Jayavelu S, Liu L, Friedl MA, Henebry GM, Liu Y, et al. Evaluation of land surface phenology from VIIRS data using time series of PhenoCam imagery. *Agricultural and Forest Meteorology*. 2018; 256:137–49.
38. Gitelson AA. Wide dynamic range vegetation index for remote quantification of biophysical characteristics of vegetation. *Journal of plant physiology*. 2004; 161(2):165–73. <https://doi.org/10.1078/0176-1617-01176> PMID: 15022830
39. Adole T, Dash J, Atkinson PM. Characterising the land surface phenology of Africa using 500 m MODIS EVI. *Applied geography*. 2018; 90:187–99.
40. Richardson AD, Hufkens K, Milliman T, Frohling S. Intercomparison of phenological transition dates derived from the PhenoCam Dataset V1. 0 and MODIS satellite remote sensing. *Scientific reports*. 2018; 8(1):1–12. <https://doi.org/10.1038/s41598-017-17765-5> PMID: 29311619
41. Lumbierres M, Méndez PF, Bustamante J, Soriguer R, Santamaría L. Modeling biomass production in seasonal wetlands using MODIS NDVI land surface phenology. *Remote Sensing*. 2017; 9(4):392.
42. Yao R, Wang L, Huang X, Guo X, Niu Z, Liu H. Investigation of urbanization effects on land surface phenology in Northeast China during 2001–2015. *Remote Sensing*. 2017; 9(1):66.
43. Liu Y, Wu C, Peng D, Xu S, Gonsamo A, Jassal RS, et al. Improved modeling of land surface phenology using MODIS land surface reflectance and temperature at evergreen needleleaf forests of central North America. *Remote Sensing of Environment*. 2016; 176:152–62.
44. Jiang Z, Huete AR, Kim Y, Didan K, editors. 2-band enhanced vegetation index without a blue band and its application to AVHRR data. *Remote Sensing and Modeling of Ecosystems for Sustainability IV*; 2007: International Society for Optics and Photonics.
45. Sakamoto T, Yokozawa M, Toritani H, Shibayama M, Ishitsuka N, Ohno H. A crop phenology detection method using time-series MODIS data. *Remote sensing of environment*. 2005; 96(3–4):366–74.
46. Boschetti M, Stroppiana D, Brivio P, Bocchi S. Multi-year monitoring of rice crop phenology through time series analysis of MODIS images. *International journal of remote sensing*. 2009; 30(18):4643–62.
47. Duchemin B, Hadria R, Erraki S, Boulet G, Maisongrande P, Chehbouni A, et al. Monitoring wheat phenology and irrigation in Central Morocco: On the use of relationships between evapotranspiration, crops coefficients, leaf area index and remotely-sensed vegetation indices. *Agricultural Water Management*. 2006; 79(1):1–27.
48. Vina A, Gitelson AA, Rundquist DC, Keydan G, Leavitt B, Schepers J. Monitoring maize (*Zea mays* L.) phenology with remote sensing. *Agronomy Journal*. 2004; 96(4):1139–47.
49. Irwin D, Irwin P. A field guide to the Natal Drakensberg. Rev. Grahamstown: Rhodes University (335p.)-illus., col. illus. ISBN; 1992.
50. Nel W. On the climate of the Drakensberg: rainfall and surface-temperature attributes, and associated geomorphic effects: University of Pretoria; 2007.
51. Henzi S, Byrne R, Whiten A. Patterns of movement by baboons in the Drakensberg mountains: primary responses to the environment. *International Journal of Primatology*. 1992; 13(6):601–29.
52. Adjorlolo C, Mutanga O, Cho MA. Estimation of canopy nitrogen concentration across C3 and C4 grasslands using WorldView-2 multispectral data. *IEEE Journal of Selected Topics in Applied Earth Observations and Remote Sensing*. 2014; 7(11):4385–92.
53. Sycholt A. A Guide to the Drakensberg: Struik; 2002.
54. Qiu S, Zhu Z, He B. Fmask 4.0: Improved cloud and cloud shadow detection in Landsats 4–8 and Sentinel-2 imagery. *Remote Sensing of Environment*. 2019; 231:111205.
55. Rouse Jr J. Monitoring the vernal advancement and retrogradation (green wave effect) of natural vegetation. 1972.
56. Jiang Z, Huete AR, Didan K, Miura T. Development of a two-band enhanced vegetation index without a blue band. *Remote sensing of Environment*. 2008; 112(10):3833–45.
57. Zhou J, Jia L, Menenti M. Reconstruction of global MODIS NDVI time series: Performance of Harmonic ANalysis of Time Series (HANTS). *Remote Sensing of Environment*. 2015; 163:217–28.

58. Wardlow BD, Egbert SL. A comparison of MODIS 250-m EVI and NDVI data for crop mapping: a case study for southwest Kansas. *International Journal of Remote Sensing*. 2010; 31(3):805–30.
59. Verhegghen A, Bontemps S, Defourny P. A global NDVI and EVI reference data set for land-surface phenology using 13 years of daily SPOT-VEGETATION observations. *International Journal of Remote Sensing*. 2014; 35(7):2440–71.
60. Rocha AV, Shaver GR. Advantages of a two band EVI calculated from solar and photosynthetically active radiation fluxes. *Agricultural and Forest Meteorology*. 2009; 149(9):1560–3.
61. Mourad R, Jaafar H, Anderson M, Gao F. Assessment of Leaf Area Index Models Using Harmonized Landsat and Sentinel-2 Surface Reflectance Data over a Semi-Arid Irrigated Landscape. *Remote Sensing*. 2020; 12(19):3121.
62. D'Allestro P, Parente C. GIS application for NDVI calculation using Landsat 8 OLI images. *International Journal of Applied Engineering Research*. 2015; 10(21):42099–102.
63. Eklundha L, Jönsson P. TIMESAT 3.3 with seasonal trend decomposition and parallel processing Software Manual. Lund University; 2017.
64. Craven P, Wahba G. Smoothing noisy data with spline functions. *Numerische mathematik*. 1978; 31(4):377–403.
65. Jönsson P, Eklundh L. TIMESAT—a program for analyzing time-series of satellite sensor data. *Computers & geosciences*. 2004; 30(8):833–45.
66. Kasuya E. On the use of  $r$  and  $r$  squared in correlation and regression. Wiley Online Library, 2019 0912–3814.
67. Gonzalez-Dugo M, Neale C, Mateos L, Kustas W, Prueger J, Anderson M, et al. A comparison of operational remote sensing-based models for estimating crop evapotranspiration. *Agricultural and Forest Meteorology*. 2009; 149(11):1843–53.
68. Posselt R, Mueller R, Stöckli R, Trentmann J. Remote sensing of solar surface radiation for climate monitoring—The CM-SAF retrieval in international comparison. *Remote Sensing of Environment*. 2012; 118:186–98.
69. Descals A, Verger A, Yin G, Peñuelas J. Improved estimates of arctic land surface phenology using Sentinel-2 time series. *Remote Sensing*. 2020; 12(22):3738.
70. Pastick NJ, Dahal D, Wylie BK, Parajuli S, Boyte SP, Wu Z. Characterizing land surface phenology and exotic annual grasses in dryland ecosystems using Landsat and Sentinel-2 data in harmony. *Remote Sensing*. 2020; 12(4):725.
71. Tian F, Cai Z, Jin H, Hufkens K, Scheifinger H, Tagesson T, et al. Calibrating vegetation phenology from Sentinel-2 using eddy covariance, PhenoCam, and PEP725 networks across Europe. *Remote Sensing of Environment*. 2021; 260:112456.
72. Eklundh L, Jönsson P. TIMESAT: A software package for time-series processing and assessment of vegetation dynamics. *Remote sensing time series*: Springer; 2015. p. 141–58.
73. Cai Z, Jönsson P, Jin H, Eklundh L. Performance of smoothing methods for reconstructing NDVI time-series and estimating vegetation phenology from MODIS data. *Remote Sensing*. 2017; 9(12):1271.
74. Li M, Liu J, editors. Reconstructing vegetation temperature condition index based on the Savitzky–Golay filter. *International Conference on Computer and Computing Technologies in Agriculture*; 2010: Springer.
75. Khobkhun B, Prayote A, Rakwatin P, Dejdumrong N, editors. Rice phenology monitoring using PIA time series MODIS imagery. 2013 10th International Conference Computer Graphics, Imaging and Visualization; 2013: IEEE.
76. Stanimirova R, Cai Z, Melaas EK, Gray JM, Eklundh L, Jönsson P, et al. An Empirical Assessment of the MODIS Land Cover Dynamics and TIMESAT Land Surface Phenology Algorithms. *Remote Sensing*. 2019; 11(19):2201.
77. Wang C, Li J, Liu Q, Zhong B, Wu S, Xia C. Analysis of Differences in Phenology Extracted from the Enhanced Vegetation Index and the Leaf Area Index. *Sensors*. 2017; 17(9):1982. <https://doi.org/10.3390/s17091982> PMID: 28867773
78. Zhang Y, Hepner GF. Short-Term Phenological Predictions of Vegetation Abundance Using Multivariate Adaptive Regression Splines in the Upper Colorado River Basin. *Earth Interactions*. 2017; 21(1):1–26.
79. Wang S, Lu X, Cheng X, Li X, Peichl M, Mammarella I. Limitations and challenges of MODIS-derived phenological metrics across different landscapes in pan-Arctic regions. *Remote Sensing*. 2018; 10(11):1784.
80. Peng D, Wang Y, Xian G, Huete AR, Huang W, Shen M, et al. Investigation of land surface phenology detections in shrublands using multiple scale satellite data. *Remote Sensing of Environment*. 2021; 252:112133.

81. Huete A, Didan K, Miura T, Rodriguez EP, Gao X, Ferreira LG. Overview of the radiometric and biophysical performance of the MODIS vegetation indices. *Remote sensing of environment*. 2002; 83(1–2):195–213.
82. Testa S, Soudani K, Boschetti L, Mondino EB. MODIS-derived EVI, NDVI and WDRVI time series to estimate phenological metrics in French deciduous forests. *International journal of applied earth observation and geoinformation*. 2018; 64:132–44.
83. Davi H, Soudani K, Deckx T, Dufrene E, Le Dantec V, Francois C. Estimation of forest leaf area index from SPOT imagery using NDVI distribution over forest stands. *International Journal of Remote Sensing*. 2006; 27(05):885–902.
84. Soudani K, François C, Le Maire G, Le Dantec V, Dufrêne E. Comparative analysis of IKONOS, SPOT, and ETM+ data for leaf area index estimation in temperate coniferous and deciduous forest stands. *Remote sensing of environment*. 2006; 102(1–2):161–75.
85. Zuo L, Liu R, Liu Y, Shang R. Effect of Mathematical Expression of Vegetation Indices on the Estimation of Phenology Trends from Satellite Data. *Chinese Geographical Science*. 2019; 29(5):756–67.
86. Zhao H, Yang Z, Li L, Di L. Improvement and comparative analysis of indices of crop growth condition monitoring by remote sensing. *Transactions of the Chinese Society of Agricultural Engineering*. 2011; 27(1):243–9.
87. Pettorelli N, Vik JO, Mysterud A, Gaillard J-M, Tucker CJ, Stenseth NC. Using the satellite-derived NDVI to assess ecological responses to environmental change. *Trends in ecology & evolution*. 2005; 20(9):503–10. <https://doi.org/10.1016/j.tree.2005.05.011> PMID: 16701427
88. Schneider LC. Bracken fern invasion in southern yucatán: a case for land-change science. *Geographical Review*. 2004; 94(2):229–41.
89. Marrs R, Le Duc M, Mitchell R, Goddard D, Paterson S, Pakeman R. The ecology of bracken: its role in succession and implications for control. *Annals of Botany*. 2000; 85:3–15.
90. Dawson TP, Jackson ST, House JI, Prentice IC, Mace GM. Beyond predictions: biodiversity conservation in a changing climate. *science*. 2011; 332(6025):53–8. <https://doi.org/10.1126/science.1200303> PMID: 21454781
91. Douterlungne D, Levy-Tacher SI, Golicher DJ, Dañobeytia FR. Applying indigenous knowledge to the restoration of degraded tropical rain forest clearings dominated by bracken fern. *Restoration Ecology*. 2010; 18(3):322–9.
92. Levy-Tacher S, Vleut I, Román-Dañobeytia F, Aronson J. Natural regeneration after long-term bracken fern control with balsa (*Ochroma pyramidale*) in the Neotropics. *Forests*. 2015; 6(6):2163–77.